Innovative Piperidine-Catalyzation in Protecting Carbonyl Compounds with Implications for Angiogenesis and Inflammation

Mukhlif Mohsin Slaihim[1*], Luay Ali Dhahi [2], and Abeer Hussein Ali [3]

Abstract

Introduction: This study explores the application of piperidine-catalyzed protection, an innovative technique, for safeguarding various carbonyl compounds functioning as acetals in a generic reaction. Specifically, we investigate the catalysis of 2-amino-1,3-propanediol-2-methyl with various aromatic aldehydes, leading to the production of cis and trans-5-methyl-2-(mono or di-substitutions-phenyl)-1,3-dioxane-5-amine. Methods: Identification of all newly formed products is achieved through the utilization of spectroscopic techniques, including IR, 1H-NMR, and 13C-NMR spectroscopy. Molecular interactions and potential therapeutic applications of compounds E1 and E2 are demonstrated with cAMP-specific phosphodiesterase (1zkl) and oxidized purine nucleoside triphosphate hydrolase (5ws7). Detailed structural analyses highlight specific hydrogen bonds, pi-pi stacked interactions, and alkyl contacts formed by these compounds with target proteins. A comprehensive bioinformatics approach molecular functions, and cellular components associated with the compounds. Results: Compounds E1 and E2 exhibit diverse enrichment profiles, suggesting their involvement in various signaling cascades, involves GO enrichment, STRING protein-protein association networks, KEGG pathway analysis, and Reactome pathways to elucidate biological processes, neurotransmission, immune responses, and cancer pathways. Comparative analysis of five compound pairs (A1/A2, B1/B2, C1/C2, D1/D2, E1/E2) reveals subtle distinctions in enrichment patterns, implying unique pharmacological advantages for each pair. Conclusion: This study introduces a separate investigation on piperidine-catalyzed protection of carbonyl groups in aldehydes, presenting a practical approach. Emphasizing the significance of understanding distinct biological signatures, our findings guide therapeutic applications and compound optimization, particularly in the context of anti-cancer therapeutics. The compounds show potential in modulating neuronal function, neurotransmission, cancer mechanisms, and immune responses, suggesting promising avenues for future research and development.

Significance | Introduced piperidine-catalyzed protection in aldehydes, guiding anti-cancer compound optimization.

*Correspondence: Mukhlif Mohsin Slaihim
College of Applied Sciences, University of Samarra, Iraq
Email: mukhlif.m.s@uosamarra.edu.iq

1. Introduction

In carbohydrate chemistry, organic and pharmaceutical compounds, as well as drug design chemistry, and protecting carbonylated groups are crucial (Memon et al., 2015). Therefore, a lot of scientific research tended towards finding suitable protection groups. Despite these initiatives, protecting 1,3-dioxolane and 1,3-dioxane remains the most sensible option

(Krompiec et al., 2012). The simplicity of the protection process and the simple accessibility of the starting compounds are the apparent reasons for this selection (Clerici et al., 2001). Acetals and ketal-type molecules could be utilized to completely synthesize natural molecules, making them useful intermediates in the synthesis of organic compounds (Ott et al., 1989). For the carbonyl group protection procedure, certain types of acid acids or catalysts are normally required (Corma and Garcia, 2003). The limitations are due to non-chemo selectively and compatibility with the various other functional groups in the molecule. The two fundamental issues with existing defensive strategies are the slow reaction times and the conditions, which need a high temperature and a stoichiometric amount of molecules. Developing a new technique that can addresses these problems and to be utilized in a catalytic process with various substrates is a desirable outcome (Mahrwald, 1994; Kshirsagar et al., 2010; Beregszászi and Molnár, 1997; Boukachabia et al., 2022; Pério et al., 1997; Karimi et al., 1999; Torok et al., 1993). Many of the currently employed procedures frequently employ trifluoromethane sulfonic acid, trifluoromethane sulfonic anhydride, boron trifluoride etherate, and other toxic and caustic chemicals. Furthermore, it has been shown under the right conditions that lanthanides and other metal catalysts excel in selectively catalyzing most carbonyl compounds. Lanthanides are substrate-specific, so it is not possible to use these catalysts as a general protection strategy. Therefore, a different approach that may address these issues and be used in a catalytic process with a variety of substrates is greatly desired. Iodine-catalyzed organic conversions were investigated prior to this work in 2005. The authors' research has expanded to include the preservation of carbonyl groups. Iodine-catalyzed reactions hold a lot of potential. The scientists presented a preliminary overview of the molecular iodine-mediated synthesis of metals in their research. They reported that the synthesis of highly selective cis and trans dioxolanone derivatives was achieved through the same-condition reactions of mandelic acid and lactic acid with a number of aldehydes (Banik et al., 2005). However, for the protection of the carbonyl group of the para-nitro benzaldehyde used in our study in the presence of piperidine, the first experiment yielded a combination of Schiff bases and the derivative 1, 3-dioxane.

On the other hand, the 1,3-dioxane derivative formed a racemic pattern in that experiment due to the carbonyl group's protection, and the racemic mixture was simple to separate from the Schiff base. In our current study, we used piperidine as a catalyst and amino-2-methylpropane-1, 3-diol to protect the carbonyl groups of a new series of benzaldehyde derivatives.

As for the potential biological effects of these compounds and their importance in the field of drug design, one of a major obstacle to a successful chemotherapy of cancer is multidrug resistance (MDR) to antitumor agents. It seems that the fundamental factor responsible for MDR is overexpression of P-glycoprotein (p-gp) (Duan et al., 2023). Further, It has been reported that in a few research, unique aromatic core structures of 2,2-diphenyl-1,3-dioxolane and 2,2-diphenyl-1,3-dioxane derivatives were synthesized, evaluated, and shown to have high MDR reversal activity in human Caco-2 cells (Schmidt et al., 2007).

Finally, derivatives of 1,3-dioxane ring are involved in industrial processes as reagents in accurate organic synthesis (Haque et al., 2013).They also were evaluated biologically active molecules with anti-inflammatory, antifungal, antibacterial properties, and reported as effective modulators of multidrug resistance (Zeng et al., 2015). Within this class of compounds, a substitutions at positions 2 and 5 of the 1,3-dioxane molecule have been considered for their major potential in terms of structural variety (Wong et al., 2004; Arafath et al., 2017).

3. Materials and Methods

3.1. Chemicals and instruments

Chemicals: The following materials and reagents were utilized for all the synthesized compounds: 4-Nitrobenzaldehyde (BDH); 2-Bromobenzaldehyde (BDH); Piperidine (BDH); Dimethyl sulfoxide (Merck); 2-amino-2-methyl-1,3-propanediol (Sigma, China); 4-Chlorobenzaldehyde (BDH); 4-Bromobenzaldehyde (BDH); 2,4-Dichlorobenzaldehyde (BDH). Aluminum sheets of TLC silica gel 60 F254, 20cm x 20cm (Merck, Germany) were used.

Instruments: All equipment or tools required to ascertain the chemical composition of generated substances, except a Bruker Advance, are housed at Samarra University's College of Applied Sciences. At Basra University's College of Education, Department of Chemistry, nuclear magnetic resonance (^{1}H-NMR) and ^{13}C-NMR spectra were measured using a Bruker Advance (400 MHz) and DMSO-d6 solvent. Fourier Transform Infrared Spectrophotometer/FTIR-8400S provided by Shimadzu Japanese Company was used to capture infrared spectra; samples were made into (KBr) discs. Mass spectra were obtained using the Shimadzu GC-MS-QP 2010 Ultra mass spectrometer. The German manufacturer Sartorius' delicate Balance was used. Melting Point Digital Advanced SMP30 supplied by the Stuart-United Kingdom was utilised and all melting points apparatus are uncorrected.

3.2. General procedure for the synthesis of *Cis* and *Trans*-5-methyl-2-(mono or di-substitutions-phenyl)-1, 3-dioxane-5-amine (A1–E1 & A2–E2)

To create a new mixture of *Cis* and *Trans*-5-methyl-2-(mono or di-substitutions-phenyl)-1,3-dioxane-5-amine **(A1-E1)** and **(A2-E2)** respectively, piperidine (0.5 mL) was mixed with an equimolar amount of 2-amino-2-methyl-1,3-propanediol (0.001 mol) and one of the aromatic aldehyde derivatives. The contents of the

reaction were stirred and refluxed for six hours. It is then concentrated and given time to gradually cool. The precipitate was filtered, dried, and purified using column chromatography.

3.3. Identifying pharmacokinetic properties:

The 2D structures of the proposed compounds were drawn using ChemSketch software and optimized to generate 3D geometries, then saved in .mol2 format. These mol2 files were uploaded to the SwissADME web server, which calculates physicochemical parameters and pharmacokinetic properties. SwissADME implements predictive models including physicochemical filters, brain penetration, oral bioavailability, lipophilicity, solubility, medicinal chemistry friendliness, and synthesizability. The outputs for each compound were extracted to compile the pharmacokinetic profile (Table 3).

3.4. Predicting biological targets:

Putative protein targets were predicted using three complementary in silico target prediction platforms - SwissTargetPrediction, SEA, and SuperPred. For SwissTargetPrediction, the simplified molecular-input line-entry system (SMILES) strings were inputted and targets were predicted based on 2D and 3D similarity ensemble approaches. For SEA, the .mol2 files were uploaded and amino acid sequence-order independent pocket-based 3D similarity algorithm was applied. For SuperPred, .sdf files were submitted and targets were predicted based on structural similarity and machine learning models. The top predicted targets from each platform were compared to derive a set of high confidence putative targets for each compound.

3.5. Validating and filtering predicted targets using molecular docking:

Molecular docking using AutoDock Vina 1.2.5 was performed to validate and prioritize predicted protein targets. The 3D structures of predicted targets were retrieved from the Protein Data Bank (PDB). Compound structures were optimized and converted to .pdbqt format. Receptors were prepared by removing ligands, adding polar hydrogens and charges, and converting to .pdbqt format. A grid box was defined around the binding site for each receptor. Compounds were docked flexibly using exhaustiveness set to 20. The accepted binding affinity scores cutoff was set to be ≤-6 (Alshehade et al., 2022).

3.6. Multi-omic enrichment analysis

The selected predicted protein targets for each compound were input into the Enrichr web tool for enrichment analysis (Eid et al., 2023). Gene Ontology databases for Biological Process, Molecular Function, and Cellular Component were queried against the target lists to identify overrepresented ontologies. The Search Tool for the Retrieval of Interacting Genes/Proteins (STRING) was used to derive protein-protein interaction networks and clusters. Kyoto Encyclopedia of Genes and Genomes (KEGG) pathway analysis was performed to identify enriched pathways. Reactome pathway

knowledgebase was searched to find enriched pathways and reactions. DISEASES was utilized to determine disease associations based on the input genes. For each database query, enrichment was considered significant at adjusted p-value < 0.05. The enriched terms and pathways were compared across compounds to derive biological signatures and therapeutic implications.

2. Results and discussion

2.1. Chemistry of 1,3-dioxane derivatives

All new 1,3-dioxane derivatives were synthesized via reaction between the some substituted aromatic aldehyde and 2-amino-2-methyl-1,3-propanediol. Moreover, the substituted aromatic aldehydes by electron withdrawing groups go through a carbonyl group protection reaction in the presence of piperidine ,and 1,3-dioxane derivatives were obtained as finally resuls. Some substituted aromatic aldehydes by electron donating groups like 4-methyl benzaldehyde,4-methyl benzaldehyde, 4-methoxy benzaldehyde, and $4\text{-}(CH_3)_2N$-benzaldehyde are examples of aldehydes that do not go through the carbonyl group protection procedure, despite the fact that some aldehydes do not respond well to the carbonyl group protection process and have a strong potential to produce Schiff base derivatives (Khairuddean et al., 2020; Slaihim et al., 2019; Slaihim et al., 2023).

The unprocessed reaction mixture was treated to separate the Schiff base derivatives from this 1,3-dioxane derivative, which was likewise generated as a mixture of *Cis-* and *Trans*-isomers. These 1,3-dioxane derivatives are created by the combination of their *Cis-* and *Trans*-isomers. By using ^{1}H-NMR and ^{13}C-NMR spectroscopy, the resulting 1,3-dioxane derivative was properly identified and had a good yield. The scheme 1 below shows how the carbonyl group protection method used in this study produced a mixture of *Cis* and *trans*-1,3-dioxane derivatives:

The (**Scheme 2**) below shows suggested mechanism of carbonyl groups protection reaction through utilizing the piperidine as new catalyst to produce 1,3-dioxane derivatives:

2.2. Characterisation of 1,3-dioxane derivatives

IR & ^{1}H-NMR data for the *cis* and *trans* series of 1, 3-dioxane are displayed in (**Table 1**) & (**Table 2**) respectively, and the physical properties of the 1, 3-Dioxan series are provided in (**Table 5**). The carbonyl groups of the selected benzaldehyde derivatives and the two hydroxyl groups of the 1,3-diol substance vanished from the infrared spectra of all *cis* and *trans*-1,3-dioxane derivatives (**Figure 1**). Due to the methyl groups in the trans and cis derivatives of 1,3-dioxane, respectively, all ^{1}H-NMR spectra showed monomeric signals in the region of chemical shift **1.08–1.15 ppm** and other signals in the range of chemical shift **1.14–1.19 ppm**. Additionally, all of the compounds' spectra showed monomeric signals at chemical shifts between **3.37 and 3.43 ppm**
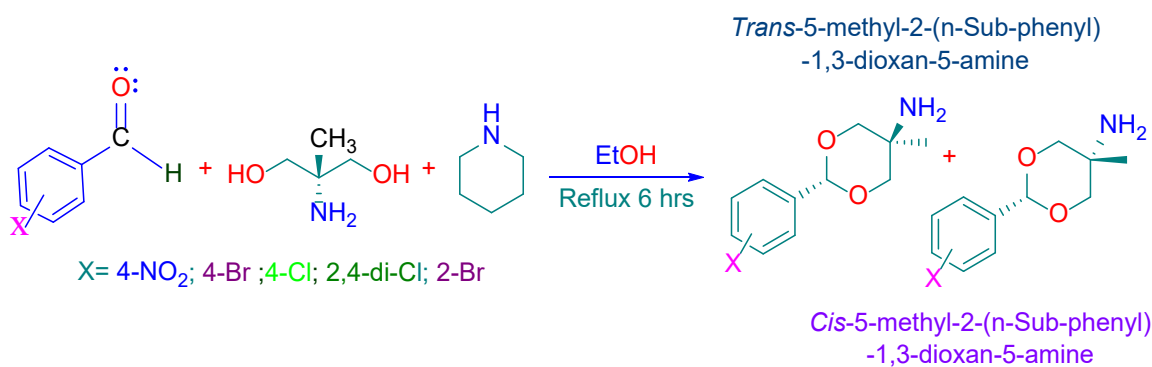
Scheme 1. The general preparation process for *Cis* and *Trans*-1, 3-dioxane series
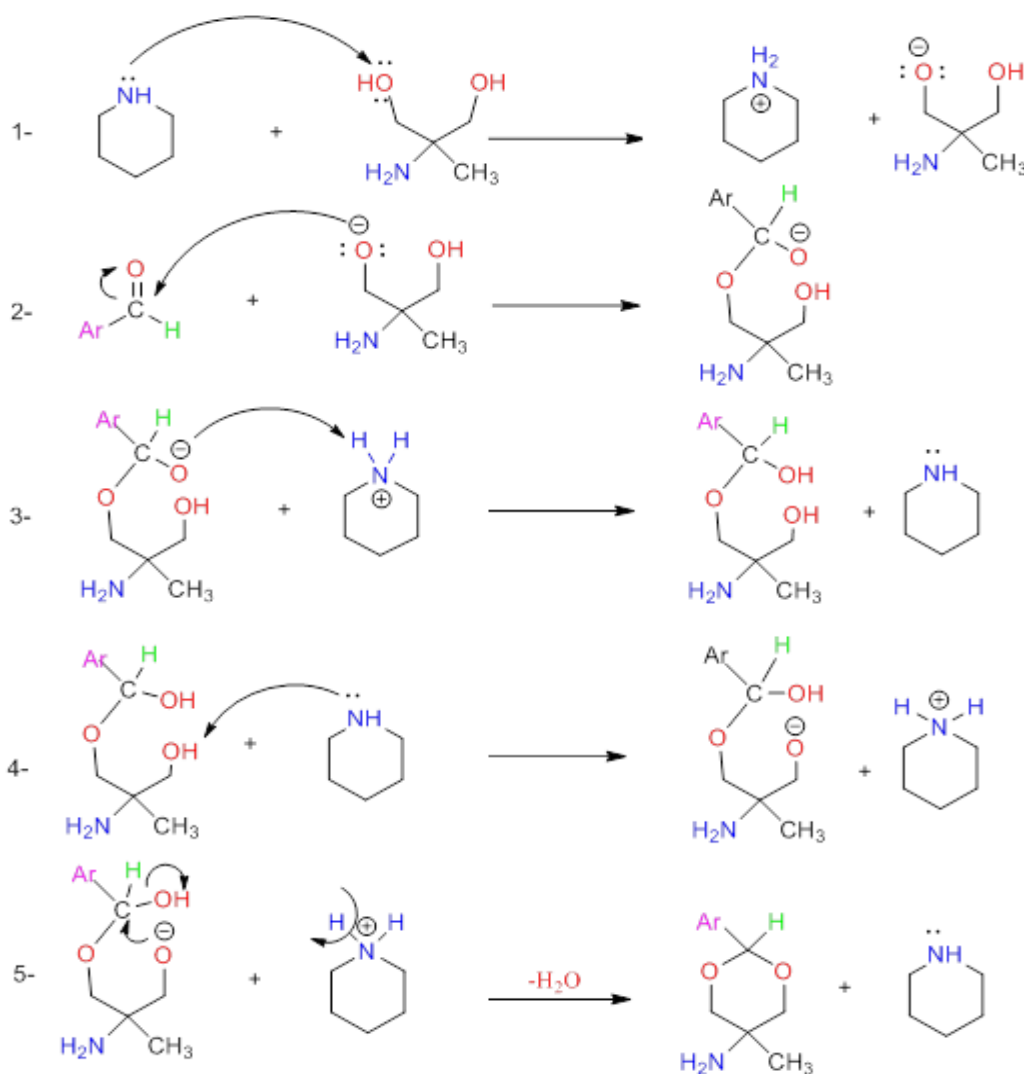
Scheme 2. Mechanism of the piperidine-catalysed of carbonyl group protection.

Table 1. IR Data of *Cis* and *Trans*-1, 3-dioxane series

Comp No	N-sub-phenyl	(C=C)$_{Ar}$	(C-H)$_{Ar}$	(-NH$_2$)	(-CH$_3$)	(C-O-C)st sy ; (C-O-C)st as	(O-CH2) st as	Other
A1 & A2	4-NO2-Ph	1605;1483	3115	3264; 3237	2967; 2874	1061; 856	1109	(C-NO2) st sy: 1346 ;(C-NO2) st sy: 1518
B1 & B2	4-Br-Ph	1597;1477	3100	3250; 3150	2922; 2882	1060; 822	1125	
C1 & C2	4-Cl-Ph	1597;1473	3101	3250; 3185	2930; 2880	1070; 822	1120	
D1 & D2	2,4-DiCl-Ph	1589;1464	3101	3258; 3160	2933; 2876	1082; 856	1122	
E1 & E2	2-Br-Ph	1609;1467	3102	3268; 3240	2932; 2876	1044; 858	1126	

Table 2. ^{1}H-NMR characteristic data of *Cis* and *Trans*-1, 3-dioxane series

Cis/ Trans			Signal Features	No. of Protons	Type of Protons
Comp. No	**Sub-Phenyl**	**Chemical Shift (δ) ppm**			
A1&A2	**4-NO2-Ph**	1.16/ 1.08	s	3H	-CH$_3$
		3.27/ 3.26	s	2H	-NH$_2$
		3.33/ 3.42	d, J = 8.0 Hz	2H$_{eq}$	(-CH$_2$)$_{4,6}$ of 1,3-dioxane ring (2H$_{eq}$)
		3.36/ 3.81	dd, J = 4.0 Hz	2H$_{ax}$	(-CH$_2$)$_{4',6'}$ of 1,3-dioxane ring (2H$_{ax}$)
		4.94/ 5.58	s	1H	(-CH) of 1,3-dioxane ring
		7.71/ 7.70	d, J = 8.0 Hz	2H	(-CH)$_{2,6}$ of Phenyl ring
		8.24/ 8.23	d, J = 8.0 Hz	2H	(-CH)$_{3,5}$ of Phenyl ring
B1&B2	**4-Br-Ph**	1.14/ 1.13	s	3H	-CH$_3$
		3.33/ 3.32	s	2H	-NH$_2$
		3.35/ 3.40	d, J = 8.0 Hz	2H$_{eq}$	(-CH$_2$)$_{4,6}$ of 1,3-dioxane ring (2H$_{eq}$)
		3.37/ 3.78	dd, J = 4.0 Hz	2H$_{ax}$	(-CH$_2$)$_{4',6'}$ of 1,3-dioxane ring (2H$_{ax}$)
		5.43/ 5.42	s	1H	(-CH) of 1,3-dioxane ring
		7.44/ 7.42	d, J = 8.0 Hz	2H	(-CH)$_{2,6}$ of Phenyl ring
		7.46/ 7.45	d, J = 8.0 Hz	2H	(-CH)$_{3,5}$ of Phenyl ring
C1&C2	**4-Cl-Ph**	1.15/ 1.14	s	3H	-CH$_3$
		3.35/ 3.34	s	2H	-NH$_2$
		3.36/ 3. 42	d, J = 8.0 Hz	2H$_{eq}$	(-CH$_2$)$_{4,6}$ of 1,3-dioxane ring (2H$_{eq}$)
		3.40/ 3.80	dd, J = 4.0 Hz	2H$_{ax}$	(-CH$_2$)$_{4',6'}$ of 1,3-dioxane ring (2H$_{ax}$)
		5.43/ 5.42	s	1H	(-CH) of 1,3-dioxane ring
		7.41/ 7.39	d, J = 8.0 Hz	2H	(-CH)$_{2,6}$ of Phenyl ring
		7.42/ 7.40	d, J = 8.0 Hz	2H	(-CH)$_{3,5}$ of Phenyl ring
D1&D2	**2,4-Di Cl-Ph**	1.17/ 1.15	s	3H	-CH$_3$
		3.34/ 3.33	s	2H	-NH$_2$
		3.36/ 3. 42	d, J = 8.0 Hz	2H$_{eq}$	(-CH$_2$)$_{4,6}$ of 1,3-dioxane ring (2H$_{eq}$)
		3.40/ 3.89	dd, J = 4.0 Hz	2H$_{ax}$	(-CH$_2$)$_{4',6'}$ of 1,3-dioxane ring (2H$_{ax}$)
		5.68/ 5.67	s	1H	(-CH) of 1,3-dioxane ring
		7.58/ 7.57	dd	1H	(-CH)$_6$ of Phenyl ring
		7.65/ 7.64	s	1H	(-CH)$_3$ of Phenyl ring
		7.67/ 7.66	d	1H	(-CH)$_5$ of Phenyl ring
E1&E2	**2-Br-Ph**	1.19/ 1.14	s	3H	-CH$_3$
		3.43/ 3.42	s	2H	-NH$_2$
		3.34/ 3. 45	d, J = 8.0 Hz	2H$_{eq}$	(-CH$_2$)$_{4,6}$ of 1,3-dioxane ring (2H$_{eq}$)
		3.38/ 3.83	dd, J = 4.0 Hz	2H$_{ax}$	(-CH$_2$)$_{4',6'}$ of 1,3-dioxane ring (2H$_{ax}$)
		5.64/ 5.62	s	1H	(-CH) of 1,3-dioxane ring
		7.26-7.31	m	1H	(-CH)$_6$ of Phenyl ring
		7.35-7.41	m	1H	(-CH)$_3$ of Phenyl ring
		7.57-7.64	m	2H	(-CH)$_{4,5}$ of Phenyl ring

and additional signals at chemical shifts between **3.26 and 3.34 ppm** that belonged to the amino groups of the derivatives of *cis* and *trans*-1,3-dioxane, respectively. Regarding the -CH$_2$- groups in cis-1,3-dioxane derivatives, they showed up as two doublet signals with an abundance of two protons each, one in the chemical shift range **3.36-3.33 ppm** and the second in the chemical shift range **3.40-3.36 ppm**. While the -CH$_2$- groups showed up in trans-1,3-dioxane derivatives as four doublet signals, two of them were superimposed with an abundance of two protons that were located in the high field at a chemical shift range of **3.78–3.40 ppm**, and two of them were superimposed with an abundance of two protons that were located in the downfield at a chemical shift range of **3.89–3.43 ppm**. Furthermore, singlet signals with chemical shifts ranging from **5.68 to 4.94 ppm** were visible in the area of all ^{1}H-NMR spectra, as well as a relative abundance of one proton per -CH- group in both the cis and trans derivatives of 1,3-dioxane. The protons of the phenyl ring show superimposed doublet signals for para-substituted phenyl rings at the chemical shift of **8.24–7.26 ppm** in both the cis and trans forms of the 1,3-dioxane derivatives **(Figure 2)**. According to the ^{13}C-NMR spectra, both the cis and trans-1,3-Dioxane derivatives' anticipated signals were present. Except for two signals that belonged to the derivative of cis-1,3-dioxane, the majority of the signals in the ^{13}C-NMR spectra of the combination of cis and trans-1,3-dioxane were neighboring. The presence of four fundamental kinds of proton-carrying carbon signals in the ^{13}C-NMR spectra served as the defining characteristic of all spectra (Marucci et al., 2005). The aliphatic and aromatic tetracarbon atoms appeared in the chemical displacement ranges of **63.80-65.61 ppm** and **128.77-149.06 ppm**, respectively, while the signals of the methyl group appeared at **22.15-22.76 ppm**, the signals of the -CH- group appeared at **88.17-91.48 ppm**, and the signals of the -CH$_2$- group appeared at **73.10-73.41 ppm**. Despite the signals of the Ar-H protons appearing at **123.88-129.18 ppm (Figure 3)**.

2.3 The pharmacokinetic properties of the proposed compounds

The pharmacokinetic properties of drug compounds (Table 2) play a critical role in determining their efficacy, safety, and developmental viability. An analysis of the pharmacokinetic properties of the 5 compounds A-E and their cis and trans isomers reveals both similarities and key differences. Compounds A1/A2, which are geometric isomers, have identical pharmacokinetic parameters as expected. The same pattern holds for the other 4 compound pairs B1/B2, C1/C2, D1/D2, and E1/E2. In general, the compounds exhibit high gastrointestinal absorption, no inhibition of major cytochrome P450 enzymes, and follow Lipinski's guidelines for drug-likeness. However, blood-brain barrier permeability differs. While compounds A1/A2 show poor BBB permeation, the other 8 compounds are predicted to readily cross the BBB. This difference may be attributed to the pyrrolidine ring in A1/A2 which increases polarity. The compounds also differ in synthetic accessibility with A1/A2 being more complex to synthesize than the others. While geometric isomers within each pair have identical pharmacokinetic profiles, notable differences exist between the 5 scaffolds. The choice of optimal compound would depend on the desired pharmacokinetics. For treating systemic conditions, B-E may be preferred over A1/A2 due to their improved BBB permeation. However, for gastrointestinal or peripheral conditions, A1/A2 may offer advantages. Careful consideration of pharmacokinetic factors in early development can assist in selecting promising lead compounds.

2.4 Biological enrichment analysis of the predicted target of the proposed compounds

A multi-pronged in silico approach was utilized to gain insights into the biological targets and molecular mechanisms of action of the 10 compounds under study. Computational target prediction was performed using SwissTargetPrediction, the similarity ensemble approach (SEA), and SuperPred, revealing a total of 258 potential protein targets. To refine this large set of predictions, molecular docking studies were carried out. Using a stringent binding affinity cutoff of -6 kcal/mol, 102-159 high confidence predicted targets were obtained for each compound (Figure 4). For instance, compound C2 was predicted to bind 128 targets, providing clues into its broad biological activities and multi-targeted mechanisms inferred from enrichment analysis. Overall, this rigorous workflow combining target prediction and molecular docking generated novel hypotheses and high-quality target sets for further experimental testing. The identification of 149 and 159 targets for compounds A1 and A2 demonstrates their potential for polypharmacological effects. In contrast, compounds B1 and B2 had fewer predicted targets at 82 and 103 respectively, suggesting more selective pharmacological profiles. By strengthening target prediction through molecular modeling, this study significantly enhanced understanding of the biological and molecular activities of these functionally diverse small molecule compounds. The predicted target profiles provide a foundation to guide future mechanistic studies and exploration of therapeutic applications.

The docking results revealed a diverse set of top-scoring protein targets (Table 3) for the various compounds (A1, A2, B1, etc), with predicted binding affinities ranging from -7.7 to -8.5 kcal/mol. While A1 preferred more polar residues like serines and asparagines in proteins such as cAMP phosphodiesterase and serotonin transporter, hydrophobic contacts dominated for B1 with glycogen synthase kinase-3 beta and nitric oxide synthase 3 (Table 4).

Table 3. Pharmacokinetic properties of drug compounds

Molecule	A1	A2	B1	B2	C1	C2	D1	D2	E1	E2
Formula	C11H14N2O4	C11H14N2O4	C11H14BrNO2	C11H14BrNO2	C11H14ClNO2	C11H14ClNO2	C11H13Cl2NO2	C11H13Cl2NO2	C11H14BrNO2	C11H14BrNO2
MW	238.24	238.24	272.14	272.14	227.69	227.69	262.13	262.13	272.14	272.14
#Heavy atoms	17	17	15	15	15	15	16	16	15	15
#Aromatic heavy atoms	6	6	6	6	6	6	6	6	6	6
#Rotatable bonds	2	2	1	1	1	1	1	1	1	1
#H-bond acceptors	5	5	3	3	3	3	3	3	3	3
#H-bond donors	1	1	1	1	1	1	1	1	1	1
MR	62.26	62.26	61.14	61.14	58.45	58.45	63.46	63.46	61.14	61.14
TPSA	90.3	90.3	44.48	44.48	44.48	44.48	44.48	44.48	44.48	44.48
WLOGP	1.03	1.03	1.89	1.89	1.78	1.78	2.43	2.43	1.89	1.89
GI absorption	High	High	High	High	High	High	High	High	High	High
BBB permeant	No	No	Yes	Yes	Yes	Yes	Yes	Yes	Yes	Yes
Pgp substrate	No	No	No	No	No	No	No	No	No	No
CYP1A2 inhibitor	No	No	No	No	No	No	No	No	No	No
CYP2C19 inhibitor	No	No	No	No	No	No	No	No	No	No
CYP2C9 inhibitor	No	No	No	No	No	No	No	No	No	No
CYP2D6 inhibitor	No	No	No	No	No	No	No	No	No	No
CYP3A4 inhibitor	No	No	No	No	No	No	No	No	No	No
Lipinski #violations	0	0	0	0	0	0	0	0	0	0
Ghose #violations	0	0	0	0	0	0	0	0	0	0
Veber #violations	0	0	0	0	0	0	0	0	0	0
Egan #violations	0	0	0	0	0	0	0	0	0	0
Muegge #violations	0	0	0	0	0	0	0	0	0	0
Bioavailability Score	0.55	0.55	0.55	0.55	0.55	0.55	0.55	0.55	0.55	0.55
Synthetic Accessibility	3.19	3.19	3.11	3.11	3.03	3.03	3.22	3.22	3.18	3.18
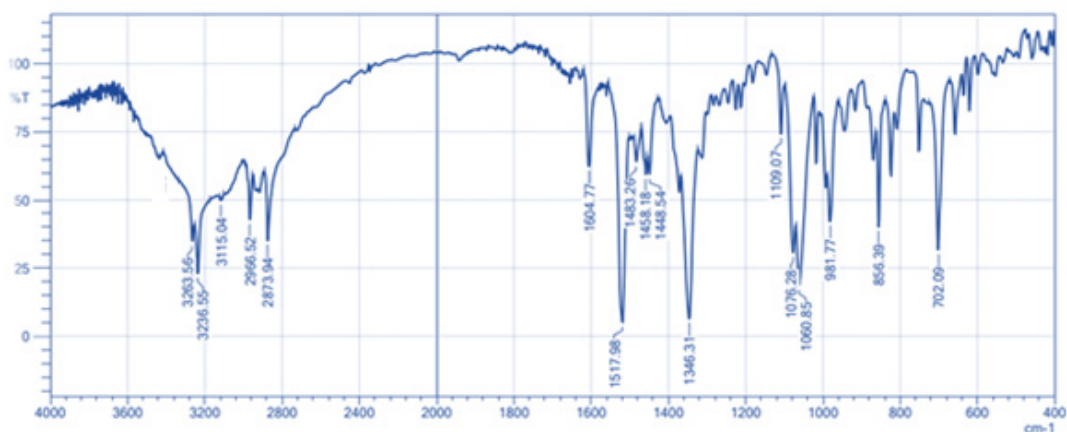
Figure 1: IR spectrum of *Cis* and *Trans* mixture A1&A2
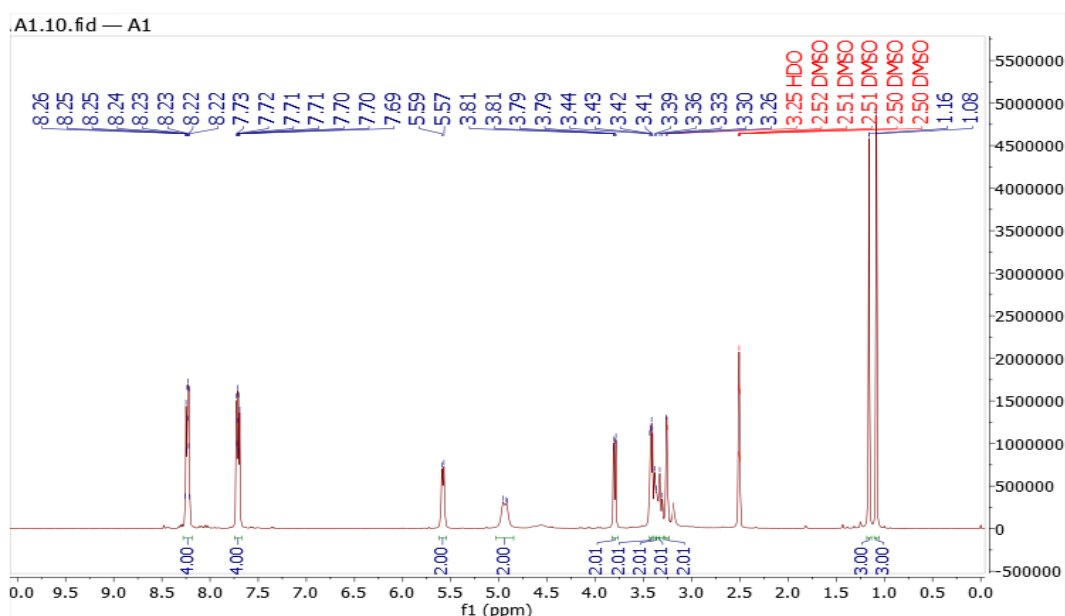
Figure 2: ¹H-NMR spectrum of *Cis* and *Trans* mixture A1&A2 (400 MHz, DMSO-d_6)
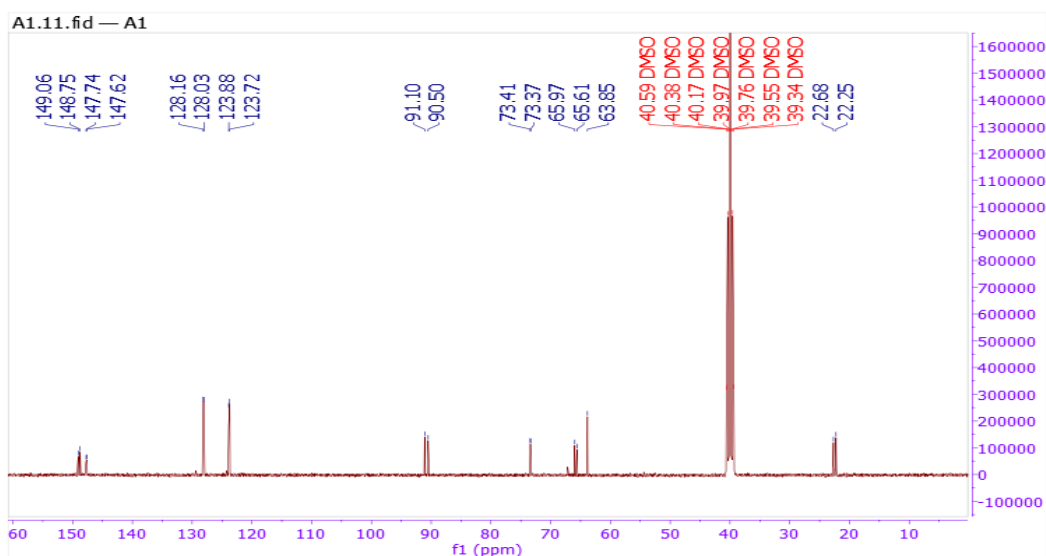
Figure 3: ¹³C-NMR spectrum of *Cis* and *Trans* mixture A1&A2 (100 MHz, DMSO-d_6)

Table 4. Top binding affinity for each compound

Target	Biological Target and PDB code	Pharmacology	Compounds	Affinity (kcal/mol)
cAMP-specific 3',5'-cyclic phosphodiesterase	(1zkl)	Inflammation	A1	-7.7
Sodium-dependent serotonin transporter	(5i6x)	Antidepressant and psychostimulant	A1	-8.1
Aldo-keto reductase family 1 member C3	(1s1p)	Inflammation and ani-cancer	A2	-7.8
Histone lysine demethylase	(3kv4)	Inflammation	A2	-7.9
Glycogen synthase kinase-3 beta	1j1b	Inflammation	B1	-7.8
Nitric oxide synthase 3	4d1p	Inflammation	B1	-7.8
Nitric oxide synthase 3	4d1p	Inflammation	B2	-7.9
Ribosyldihydronicotinamide dehydrogenase	4fgl	Inflammation	B2	-7.8
Neutrophil collagenase	1i76	Inflammation	C1	-8.1
Nitric oxide synthase 1	6cid	Inflammation	C1	-8.1
Beta-2-microglobulin	6c98	Inflammation	C2	-7.9
Nitric oxide synthase 1	6cid	Inflammation	C2	-7.9
Nitric oxide synthase 3	4d1p	Inflammation	D1	-8.2
Nitric oxide synthase 1	6cid	Inflammation	D1	-8.2
Nitric oxide synthase 3	4d1p	Inflammation	D2	-8.1
Ribosyldihydronicotinamide dehydrogenase	4fgl	Inflammation	D2	-7.9
cAMP-specific 3',5'-cyclic phosphodiesterase	1zkl	Inflammation	E1	-7.7
Oxidized purine nucleoside triphosphate hydrolase	5ws7	Inflammation	E1	-8.2
Oxidized purine nucleoside triphosphate hydrolase	5ws7	Inflammation	E2	-8.5
Soluble cytochrome b562	6bqh	Inflammation	E2	-7.9

Table 5: physical properties of 1, 3-Dioxan series

Comp No	N-sub-phenyl	Melting Point	Color	Yield%
A1 & A2	4-NO2-Ph	(81-82)°C	Light Orange	71.90%
B1 & B2	4-Br-Ph	(70-73)°C	Light Yellow	95.20%
C1 & C2	4-Cl-Ph	(76-79)°C	Off White	57.80%
D1 & D2	2,4-DiCl-Ph	(92-95)°C	Light Brown	53.80%
E1 & E2	2-Br	(62-65)°C	Yellow	51.70%
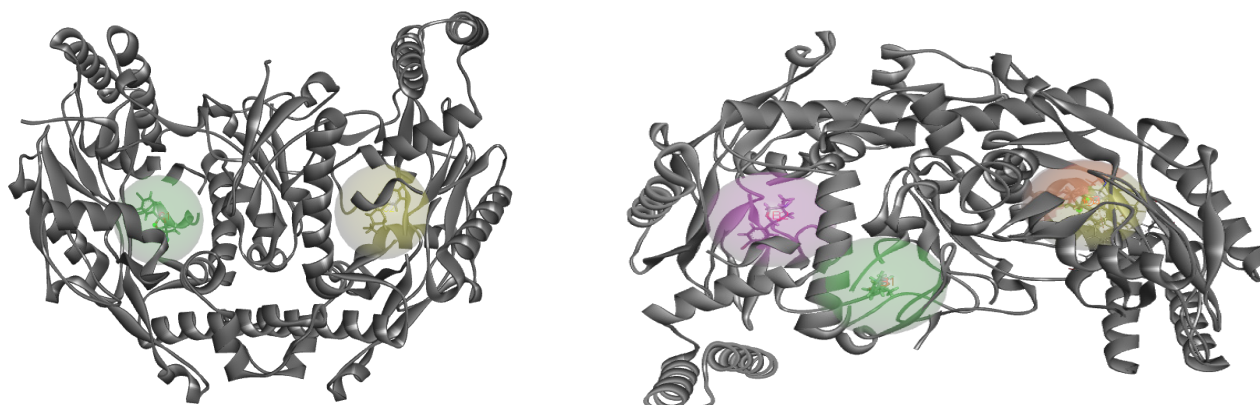
Figure 5. The active site location for C1 and C2 compounds within nitric oxide synthase 1 (ID: 6cid). The target site for B1 (green), B2 (purple), D1 (Yellow) and D2 (orange) within nitric oxide synthase 3 (ID: 4d1p)

Compounds A1 and A2

The docking studies (Table 4) revealed several notable interactions between compound A1 (cis isomer) and the sodium-dependent serotonin transporter (5i6x) and cAMP-specific phosphodiesterase (1zkl), as well as between compound A2 (trans isomer) and aldo-keto reductase (1s1p) and histone demethylase (3kv4).

With 5i6x, A1 formed conventional hydrogen bonds with residues ASN177, SER439, and SER439, along with a carbon hydrogen bond with ALA173. There were also hydrophobic pi-pi stacked and pi-alkyl interactions with TYR176 and PHE341, respectively, and a pi-alkyl interaction between A1 and ILE172. For 1zkl, two conventional hydrogen bonds occurred between A1 and residues ASP362 and GLN413, supplemented by a carbon hydrogen bond with ASP362. A1 displayed pi-pi stacked and alkyl hydrophobic interactions with PHE416 and ILE323.

In contrast, A2 made just conventional hydrogen bonds with 1s1p, interacting with ASN167, ASP50, and TYR55. A pi-pi stacked hydrophobic contact occurred between A2 and TYR216, plus a pi-alkyl association with TRP86. With 3kv4, there were no conventional hydrogen bonds, only carbon hydrogen bonds between A2 and residues ARG8, ILE248, PHE359, GLU350, and PHE359. An additional pi-donor hydrogen bond formed with PHE250. Hydrophobic interactions featured a pi-sigma contact with ARG8 and pi-pi stacked and alkyl associations with PHE250 and LEU353.

The Gene Ontology (GO) analysis indicates A1 impacts processes related to responses to stimuli, phosphorylation, and metabolism. Molecular functions include kinase activities and nucleotide binding. Enriched cellular components are the cytoplasm, cytosol, and protein kinase complexes. STRING highlights proteins involved in neurotransmitter signaling and cell cycle regulation. KEGG annotates pathways for serotonin, PI3K-Akt, and cancer. Reactome implicates GPCR signaling, synaptic transmission, and TP53 pathways. The DISEASES database associates A1 with cancer, mental health disorders, immune diseases, and substance abuse. Overall, these annotated databases link compound A1 to kinase signaling cascades, particularly those stimulated by extracellular cues like neurotransmitters and cellular stresses. There are strong indications of neuropsychiatric effects, likely via impacts on monoamine receptors and synaptic function. Cell proliferation pathways are also prominently represented, including TP53, PI3K, and cancer associations. The enrichment analysis provides a landscape of the potential biological activities of A1, spanning neuronal, immune, and cancer pathways. This information can help guide further investigations into the molecular mechanisms and therapeutic applications of this compound.

The GO enrichment analysis highlights processes related to response to stimuli, particularly oxygen-containing and organic compounds. Molecular functions enriched include catalytic, kinase, and binding activities. Cellular components like vesicles, cytoplasm, plasma membrane, and synapses are overrepresented. The STRING protein network analysis implicates proteins involved in reversible hydration of carbon dioxide and neurotransmitter disorders. KEGG pathway analysis links compound A2 to cancer, GPCR signaling, PI3K-Akt signaling, and neuroactive ligand-receptor interactions. Reactome annotates signaling events downstream of GPCRs. The DISEASES database associates A2 with cancer, mental health disorders, immune diseases, and vascular disease. In summary, these annotated databases suggest compound A2 impacts pathways regulating responses to extracellular stimuli. Kinases and stimulus-responsive membrane proteins appear centrally. There is a neuropsychiatric signature, with links to serotonin and GPCRs. Cancer and immune system effects are also indicated. This profile provides insight into the biological activities and therapeutic potential of compound A2.

Compounds B1 and B2

For glycogen synthase kinase-3 beta (1j1b), B1 engaged in conventional hydrogen bonds with residues ARG223 and ARG723 (**Supp Table 1**). There was also a conventional hydrogen bond between B1 and GLN765, plus a carbon hydrogen bond with the same residue. Electrostatic pi-cation interactions occurred between B1 and ARG223/ARG723. Hydrophobic alkyl contacts formed between B1 and ARG220/ARG720.

With nitric oxide synthase 3 (4d1p), B1 mainly showed hydrophobic interactions, featuring alkyl associations with VAL71 and VAL465. There was also a pi-alkyl contact with LEU431, supplemented by carbon hydrogen bonds with GLU463 and CYS441.

In contrast, B2 established conventional and carbon hydrogen bonds with just one residue, TRP356, in nitric oxide synthase 3 (4d1p). Hydrophobic pi-pi stacked interactions took place between B2 and TRP178/PHE353. An additional alkyl contact occurred between B2 and PRO334. For ribosyldihydronicotinamide dehydrogenase (4fgl), B2 formed a conventional hydrogen bond with ASP117 and a pi-donor hydrogen bond with TRP105. Hydrophobic pi-pi T-shaped and pi-alkyl interactions were seen between B2 and PHE126/TYR104.

The GO analysis showed overrepresentation of processes related to responses to stimuli like hormones and neurotransmitters. Molecular functions enriched included neurotransmitter receptor activities, kinase activities, and nucleotide and ion binding. Cellular components like the plasma membrane, synapses, dendrites and vesicles were overrepresented.STRING analysis identified clusters related to purinergic and prostaglandin signaling, heterotrimeric G proteins, and neurotransmitter signaling complexes. KEGG pathway analysis highlighted

involvement of neurotransmission pathways like cholinergic and serotonergic signaling. Signaling through cAMP was overrepresented, as well as cancer and viral infection pathways. Analysis with Reactome pointed to broad categories of GPCR signaling and signal transduction. Specific pathways like estrogen receptor, peptide hormone and amine neurotransmitter signaling were overrepresented. The results implicate that compound B1 likely interacts with membrane receptors and signaling components governing neuronal function, immune signaling and proliferative pathways. The putative mechanisms of action and disease associations are similar to compound B2, but B1 seems more focused on GPCRs and neurotransmission. Further studies could explore if B1 may have therapeutic value in treating neuropsychiatric or endocrine disorders.

The GO analysis showed overrepresentation of processes related to responses to stimuli, signaling, phosphorylation, and regulation of biological processes. Molecular functions enriched included kinase activities, nucleotide and ion binding, and catalytic activities. Cellular components like the plasma membrane, dendrites and protein complexes were overrepresented. STRING analysis identified clusters related to serotonin receptors, neurotransmitter disorders, amine binding, and cell cycle regulation through spindle formation. KEGG pathway analysis highlighted involvement in signaling pathways like cAMP, apoptosis, and cancer pathways. Infection-related pathways were overrepresented, as well as neurotrophin and progesterone-mediated signaling. Reactome analysis pointed to broad categories of signal transduction, GPCR signaling, synaptic transmission, and immune system processes. Specific ligand-mediated pathways like serotonin, cytokine and interleukin signaling were overrepresented. Analysis of disease associations linked the target network to mental health disorders, cancers, immune diseases and a syndrome caused by MAPK pathway dysregulation. This suggests the compound may interact with signaling pathways disrupted in proliferative, infectious and neuropsychiatric diseases.

The enrichment analyses implicate that compound B2 likely interacts with cell signaling networks, particularly kinase activities, GTPase signaling, and pathways regulating neuronal function and immune responses. The results provide insight into its putative mechanism of action and potential disease associations based on its interactome. Further studies could explore if B2 has applications in treating the implicated disorders.

Compounds C1 and C2

As shown in **Supp Table 2**, with neutrophil collagenase (1i76), C1 formed conventional and multiple carbon hydrogen bonds with PRO217. Hydrophobic pi-pi stacked interactions occurred between C1 and HIS197/TYR219. Numerous alkyl contacts took place between C1 and residues LEU193, LEU214, ILE159,

LEU160, and VAL194. There was also a pi-alkyl association with VAL194.

For nitric oxide synthase 1 (6cid), C1 displayed conventional hydrogen bonds with TRP414, CYS420, and TRP592, plus a carbon hydrogen bond with TRP592. Extensive hydrophobic pi-pi stacked contacts occurred between C1 and TRP414, PHE589, and PHE709. Alkyl interactions were seen between C1 and LEU429, ILE464, CYS420. C1 also showed several pi-alkyl associations with TRP414, PHE589, and PHE709. Figure 5 shows that C1 and C2 targeting same active site but in mirror protein monomer.

In contrast, C2 formed just one conventional hydrogen bond with beta-2-microglobulin (6c98), interacting with CYS48, along with carbon hydrogen bonds with ASP231 and GLN33. Hydrophobic pi-sigma and pi-pi stacked contacts took place between C2 and TRP176. There were also alkyl and pi-alkyl interactions between C2 and residues PRO179, ALA50.

For the same nitric oxide synthase 1 protein, C2 displayed far fewer interactions than C1, showing only a carbon hydrogen bond with GLY591. C2 maintained hydrophobic pi-pi stacked associations with TRP414 and PHE589. Alkyl contacts occurred between C2 and PRO570, LEU429, ILE464, along with pi-alkyl interactions involving TRP414, PHE589, and PHE709.

Furthermore, the GO analysis identified processes enriched in compound C1's network related to neurotransmitter and hormone signaling, including response to stimuli like hormones and neurotransmitters. Molecular functions enriched included GPCR, receptor and kinase activities. Cellular components like synaptic membranes, dendrites and receptor complexes were overrepresented. STRING analysis found clusters related to synaptic transmission, amine binding, and signaling complexes that align with the compound's apparent activity. And KEGG pathway analysis highlighted involvement of serotonergic, cholinergic and monoaminergic neurotransmission. Signaling pathways like cAMP, PI3K-Akt and MAPK were overrepresented. Links to pathways in cancer, viral infection, and immune signaling may reflect targets related to cell proliferation or inflammation. Also, analysis with the Reactome database pointed to broad categories like signal transduction, GPCR cascades, and immune signaling. Specific ligands and pathways like serotonin, dopamine and interleukin signaling were highlighted, again reflecting modulation of key neurotransmitters. Disease enrichment linked the target network to mental health disorders, cancers, immune diseases and mood disorders. This suggests the compound may interact with pathways dysregulated in these conditions. Further studies could explore if it has potential therapeutic applications.

The GO analysis revealed enrichment for processes related to responses to chemical stimuli and signaling, functions involving kinase activity and binding, and cellular components like the plasma membrane and synapses. The Search Tool for the Retrieval

of Interacting Genes/Proteins (STRING) clusters highlighted neurotransmission and serotonin receptor pathways. Kyoto Encyclopedia of Genes and Genomes (KEGG) analysis showed enrichment in serotonin signaling, cyclic AMP, neuroactive ligand-receptor interactions, and cancer pathways. Reactome pathways were enriched for G protein-coupled receptor signaling, synaptic transmission, cell cycle, and immune system processes. Analysis using the Disease Ontology database indicated associations with mental health disorders, cancer, immune diseases, and substance abuse disorders.

Overall, the results implicate that compound C1 interacts with neurotransmitter signaling pathways, likely through direct or indirect effects on receptors, signaling proteins and synaptic components. Furthermore, C2 strongly impacts neurotransmission, GPCR and kinase signaling, the cell cycle, and cancer pathways, with implications for neurological, psychiatric, and proliferative diseases. The membrane, synapse, and serotonin receptor enrichments provide clues about the compound's mechanism of action. Further studies are warranted to validate the predicted disease relationships.

Compounds D1 and D2

For nitric oxide synthase 1 (6cid), D1 engaged in conventional hydrogen bonds with residues TRP414, CYS420, and TRP592. A carbon hydrogen bond also occurred with TRP592 (**Supp Table 3**). Numerous hydrophobic pi-pi stacked interactions took place between D1 and TRP414, PHE589. Extensive alkyl associations occurred between D1 and LEU429, ILE464, CYS420. Several pi-alkyl contacts were also seen between D1 and TRP414, PHE589, PHE709.

With nitric oxide synthase 3 (4d1p), D1 displayed multiple hydrophobic pi-pi stacked interactions with TRP178 and PHE353. Alkyl contacts occurred between D1 and LEU193, ILE228, PRO334. Additional pi-alkyl associations were made between D1 and residues TRP178, PHE353, PHE473. Intersteing, the D1 and D2 targeting same active site among nitric oxide synthase 3, unlike B1 and B2, which have different active sites (Figure 5)

In contrast, D2 formed conventional hydrogen bonds with just one residue from each protein: TRP105 in ribosyldihydronicotinamide dehydrogenase (4fgl) and TRP356 in nitric oxide synthase 3 (4d1p). For 4fgl, hydrophobic pi-pi T-shaped and several pi-alkyl interactions took place between D2 and protein residues. With 4d1p, D2 showed alkyl groups with PRO334 and LEU193, along with multiple pi-alkyl contacts involving TRP178, PHE353, and PHE473.

Furthermore, the GO enrichment analysis reveals that compound D1 significantly impacts various biological processes, molecular functions, and cellular components. The processes enriched include response to stimuli like oxygen-containing compounds as well as phosphorylation and signaling events. Enriched molecular

functions consist of catalytic activities like kinase and protein binding while cellular components include neuron projections, synapses, and synaptic membranes. The STRING protein network clusters demonstrate the compound's relation to synaptic transmission, monoamine receptors, neurotransmitter disorders, and amine binding. KEGG pathway analysis implicates D1 in neuroactive ligand interactions, cAMP signaling, and serotonin synapses. Reactome highlights GPCR cascades, synaptic transmission, and cytokine signaling as enriched pathways. Finally, disease enrichment links D1 to various mental disorders, cancers, substance abuse and cardiovascular conditions. The breadth of enriched categories across databases indicates D1 is involved in neuronal signaling, synaptic plasticity, neurotransmitter activities and the pathophysiology underlying psychiatric, neurologic and substance use disorders.

The GO analysis identified enriched biological processes related to signal transduction, response to stimuli, and phosphorylation. Molecular functions like catalytic activity, kinase activity, ion binding, and nucleotide binding were overrepresented. Cellular components associated with vesicles, the plasma membrane, and the cytoplasm were enriched. The STRING protein-protein interaction clusters highlighted groups involved in synaptic transmission, GPCR signaling, and proteolysis. The KEGG pathway analysis revealed enrichment for apelin signaling, infections by Yersinia and cytomegalovirus, cancer pathways, cAMP signaling, and more. Reactome pathway analysis identified broad categories like signal transduction, neuronal system, and cytokine signaling as enriched. More specific pathways like GPCR ligand binding, interleukin signaling, and neurotransmitter synaptic transmission were overrepresented. Analysis of disease associations in DISEASES showed enrichment for mental health disorders, cardiovascular diseases, immune dysfunction, and psychosexual disorders.

Compounds E1 and E2

For cAMP-specific phosphodiesterase (1zkl), E1 engaged in conventional hydrogen bonds with residues GLN413 and ASP362. An additional carbon hydrogen bond occurred with ASP362. Hydrophobic pi-pi stacked and alkyl interactions were seen between E1 and PHE416 and ILE323 (**Supp Table 4**)

With oxidized purine nucleoside triphosphate hydrolase (5ws7), E1 displayed a conventional hydrogen bond with ASN33, supplemented by a carbon hydrogen bond with THR8. A pi-sulfur association occurred between E1 and MET81. Hydrophobic pi-pi stacked contacts took place between E1 and PHE72/TRP117. An alkyl interaction was also seen with LEU9.

In contrast, E2 showed no hydrogen bonds or electrostatic attractions with either soluble cytochrome b562 (6bqh) or 5ws7. For 6bqh, E2 exhibited hydrophobic pi-pi T-shaped interactions with PHE223, TRP324, and PHE328. Alkyl contacts occurred

between E2 and VAL135 and LEU209. With 5ws7, E2 maintained the same hydrogen bond with ASN33 and pi-sulfur association with MET81 as seen for E1. Additional hydrophobic pi-pi stacked and multiple alkyl/pi-alkyl interactions occurred between E2 and residues PHE72, TRP117, and LEU9.

Furthermore, the GO enrichment analysis identified relevant biological processes like response to oxygen compounds, signaling, and chemical stimuli. Enriched molecular functions included GPCR, amine receptor, and neurotransmitter receptor activities. Cellular components such as the plasma membrane, vesicles, cell periphery, and synapses were overrepresented. The STRING protein-protein association networks showed clusters related to synaptic transmission, monoamine receptors, and aminopeptidase complexes. KEGG pathway analysis revealed associations with cancer pathways, cAMP signaling, infections like Yersinia, and signaling events like PI3K-Akt. Reactome highlighted broad categories like signal transduction, GPCR signaling, and infectious diseases. It also identified specific cascades like PIP3-AKT and G alpha signaling. Disease Ontology (DO) enrichment linked the input genes to broad disease classes like mental disorders, cancer, and disorders of cell proliferation. Specific diseases like premature ejaculation and substance abuse disorders were enriched.

The GO enrichment analysis identified several biological processes, molecular functions, and cellular components enriched in the input gene set. Response to stimuli, signal transduction, and regulation of biological processes were among the top enriched GO biological processes. Binding, catalytic activity, and kinase activity were the most enriched molecular functions. Cellular components like vesicles, plasma membrane, and dendrites were also enriched. The STRING protein-protein interaction analysis found clusters related to amine binding, neurotransmitter disorders, aminopeptidase complexes, and heterotrimeric G-protein signaling. This suggests the input genes are involved in neurotransmission, peptide degradation, and GPCR signaling pathways. KEGG pathway analysis revealed enrichment for serotonin, cAMP, cholinergic synapse, PI3K-Akt, and other signaling pathways. Infectious disease pathways like HIV, cytomegalovirus, hepatitis B, Epstein-Barr virus, and SARS coronavirus were also enriched, highlighting the role of the input genes in immunity. Also, analysis of Reactome pathways showed enrichment for signal transduction, GPCR signaling, cell cycle, metabolism, hemostasis, and cytokine signaling events. This further supports the involvement of these genes in key signaling and regulatory processes.

Comparison of the proposed therapeutic potentials of the proposed compounds pairs

Analysis of the enrichment profiles reveals intriguing insights into the predicted biological activities and therapeutic potentials of the 5 compound pairs. While the cis and trans isomers share many common pathway associations, notable differences emerge that can guide compound optimization and selection.

The cis and trans forms of compound A demonstrate nearly identical enrichments, as expected for geometric isomers. Both strongly impact diverse signaling cascades involved in responding to extracellular stimuli and stresses. These include GTPase signaling, kinase phosphorylation, calcium signaling, and pathways governing synaptic transmission. The prominent associations with neuroactive ligand-receptor interactions, serotonin receptors, and synaptic components predict effects on neuronal function and behavior. Compound A also shows links to cancer pathways and immune system processes. This broad activity across signaling networks regulating neuronal, proliferative, and immune responses is a signature feature of A1 and A2. Their therapeutic promise likely involves modulating aberrant kinase activities in cancer or rectifying neurotransmitter and synaptic dysregulation underlying neuropsychiatric diseases.

Compounds B1 and B2 also exhibit significant overlap in their enrichment profiles, interacting with pathways governing neurotransmission, immune function, and cell proliferation. However, some subtle distinctions emerge. B1 shows greater selectivity for GPCRs and downstream cascades regulating neuronal signaling and endocrine pathways. In contrast, B2 has slightly broader impacts on kinase signaling involved in cancer mechanisms and innate immunity. This suggests B1 may have particular advantages in modulating neurotransmitter receptors and their signaling networks to treat neuropsychiatric or endocrine conditions. Meanwhile, B2's effects on cancer and immune pathways make it better suited to targeting proliferative or inflammatory disorders.

The cis and trans isomers C1 and C2 similarly modulate neurotransmission, especially serotonin receptors and signaling proteins enriched in synaptic regions. However, C2 demonstrates additional strong associations with cell cycle regulation and cancer-related signaling pathways that distinguish it from C1. The enrichments indicate C1 may be ideal for selectively targeting serotonin signaling to treat depression and anxiety disorders. On the other hand, C2's polypharmacology across serotonin receptors and cell proliferation mechanisms points to possible applications as a dual anti-cancer and psychiatric agent.

Compounds D1 and D2 also share common effects on pathways involved in neurotransmission, synaptic function, and GPCR activities based on their putative targets. However, D2 interacts with broader components regulating cytokine signaling and innate immunity compared to D1. This enriches D2's pharmacology and confers greater immunomodulatory potential. D1 seems more selectively focused on neuronal signaling. These distinctions suggest D1 may be better suited for targeting CNS disorders, while

D2 has advantages for conditions involving dysfunctional inflammatory processes.

Finally, isomers E1 and E2 exhibit extensive commonalities in their enrichment profiles, including GPCR signaling, neurotransmission, and stimulus response pathways. However, E2 demonstrates more pronounced and specific effects on hemostasis and vascular processes compared to E1. Components regulating platelet aggregation, coagulation, thrombosis, and vascular inflammation are uniquely enriched in E2 over E1. As such, E2 may have greater promise as a modulator of aberrant vascular and coagulation biology underlying thrombotic disorders.

However, the predicted protein targets and associated pathways are computational predictions that require experimental validation. The algorithms may miss relevant targets or include false positive interactions. Some key pathways modulated by the compounds could be overlooked while irrelevant pathways may be predicted. Experimental approaches like affinity chromatography, proteomics, and RNA sequencing should be used to confirm actual protein and pathway targets in living systems. Enrichment analysis also simplifies complex biology by grouping proteins into pathways. However, proteins often have pleiotropic effects and crosstalk between pathways exists. Despite these limitations, enrichment analysis provides a useful initial overview of the potential biological activities of compounds to guide further investigations. With appropriate caution regarding overinterpretation, it can yield valuable insights into mechanisms of action.

4. Conclusion

Piperidine catalyses the current, modest, and new protection of carbonyl groups of aldehydes. Several substrates can be successfully used with this approach. Carbonyl compound protective responses by diols are theoretically plausible since earlier theoretical investigations show that carbonyl compounds can react favourably with diols to produce the cis and trans-formations. This fact motivated us to approach the current investigation realistically. Furthermore, while the geometric isomers share common putative pathway effects, subtle differences in their enrichment patterns distinguish the cis and trans forms. These selective enhancements or restrictions of activity can be leveraged pharmacologically. Mapping the distinct biological signatures of each compound using enrichment analysis provides vital insights to guide therapeutic application and compound optimization efforts.

Author contribution

MMS supervised this study and designed the experiments. MMS and AHA wrote the manuscript. MMS and AHA designed and performed the experiments. LAD analyzed the results. All authors reviewed the manuscript.

Competing financial interests

The authors have no conflict of interest.

References

Alshehade, S. A., Al Zarzour, R. H., Murugaiyah, V., Lim, S. Y. M., El-Refae, H. G., & Alshawsh, M. A. (2022). Mechanism of action of Orthosiphon stamineus against non-alcoholic fatty liver disease: Insights from systems pharmacology and molecular docking approaches. Saudi Pharmaceutical Journal, 30(11), 1572-1588. https://doi.org/10.1016/j.jsps.2022.09.001

Arafath, M. A., Adam, F., Al-Suede, F. S. R., Razali, M. R., Ahamed, M. B. K., Majid, A. M. S. A., ... & Abubakar, S. (2017). Synthesis, characterization, X-ray crystal structures of heterocyclic Schiff base compounds and in vitro cholinesterase inhibition and anticancer activity. Journal of Molecular Structure, 1149, 216-228.

Banik, B. K., Chapa, M., Marquez, J., & Cardona, M. (2005). A remarkable iodine-catalyzed protection of carbonyl compounds. Tetrahedron letters, 46(13), 2341-2343.

Beregszászi, T., & Molnár, Á. (1997). Microwave-assisted acetalization of carbonyl compounds catalyzed by reusable envirocat® supported reagents. Synthetic communications, 27(21), 3705-3709.

Boukachabia, M., Bendjeffal, H., Aribi-Zouioueche, L., Riant, O., & Bouhedja, Y. (2022). Chemoselective synthesis of acyclic acetals by natural kaolin under green chemistry conditions. ChemistrySelect, 7(22), e202104610.

Clerici, A., Pastori, N., & Porta, O. (2001). Mild acetalisation of mono and dicarbonyl compounds catalysed by titanium tetrachloride. Facile synthesis of β-keto enol ethers. Tetrahedron, 57(1), 217-225.

Corma, A., & Garcia, H. (2003). Lewis acids: from conventional homogeneous to green homogeneous and heterogeneous catalysis. Chemical Reviews, 103(11), 4307-4366.

Duan, C., Yu, M., Xu, J., Li, B. Y., Zhao, Y., & Kankala, R. K. (2023). Overcoming Cancer Multi-drug Resistance (MDR): Reasons, mechanisms, nanotherapeutic solutions, and challenges. Biomedicine & Pharmacotherapy, 162, 114643.

Eid, E. E., Alshehade, S. A., Almaiman, A. A., Kamran, S., Lee, V. S., & Alshawsh, M. A. (2023). Enhancing the Anti-Leukemic Potential of Thymoquinone/Sulfobutylether-β-cyclodextrin (SBE-β-CD) Inclusion Complexes. Biomedicines, 11(7), 1891. https://doi.org/10.3390/biomedicines11071891

Haque, R. A., Iqbal, M. A., Asekunowo, P., Majid, A. A., Khadeer Ahamed, M. B., Umar, M. I., ... & Al-Suede, F. S. R. (2013). Synthesis, structure, anticancer, and antioxidant activity of para-xylyl linked bis-benzimidazolium salts and respective dinuclear Ag (I) N-heterocyclic carbene complexes (Part-II). Medicinal Chemistry Research, 22, 4663-4676.

Karimi, B., Seradj, H., & Ebrahimian, G. R. (1999). N-Bromosuccinimide (NBS) as a powerful and chemoselective catalyst for acetalization of carbonyl compounds under almost neutral reaction conditions. Synlett, 1999(09), 1456-1458.

Khairuddean, M., Slaihim, M. M., Alidmat, M. M., Al-Suede, F. S. R., Ahamed, M. B. K., Shah, A. M., & Majid, A. (2020). Synthesis, Characterisation Of Some New Schiff Base For The Piperidinium 4-Amino-5-Substituted-4h-1, 2, 4-Triazole-3-Thiolate, And Their In-Vitro Anticancer Activities. Int. J. Natural Sci. Human Sciences, 1(1), 48-58.

Krompiec, S., Penkala, M., Szczubiałka, K., & Kowalska, E. (2012). Transition metal compounds and complexes as catalysts in synthesis of acetals and orthoesters: Theoretical, mechanistic and practical aspects. Coordination Chemistry Reviews, 256(17-18), 2057-2095.

Kshirsagar, S. W., Patil, N. R., & Samant, S. D. (2010). Chemoselective Protection of Aldehydes in the Presence of Ketones Using RuPVP Complex as a Heterogeneous Catalyst. Synthetic Communications®, 40(3), 407-413.

Mahrwald, R. (1994). A Simple Procedure for the Catalytic Acetalization of Aldehydes. Journal für Praktische Chemie/Chemiker-Zeitung, 336(4), 361-362.

Marucci, G., Angeli, P., Brasili, L., Buccioni, M., Giardinà, D., Gulini, U., ... & Franchini, S. (2005). Synthesis and antimuscarinic activity of derivatives of 2-substituted-1, 3-dioxolanes. Medicinal Chemistry Research, 14, 309-331.

Memon, A. H., Ismail, Z., Al-Suede, F. S. R., Aisha, A. F., Hamil, M. S. R., Saeed, M. A. A., ... & Majid, A. M. S. A. (2015). Isolation, characterization, crystal structure elucidation of two flavanones and simultaneous RP-HPLC determination of five major compounds from Syzygium campanulatum Korth. Molecules, 20(8), 14212-14233.

Ott, J., Tombo, G. R., Schmid, B., Venanzi, L. M., Wang, G., & Ward, T. R. (1989). A versatile rhodium catalyst for acetalization reactions under mild conditions. Tetrahedron letters, 30(45), 6151-6154.

Pério, B., Dozias, M. J., & Hamelin, J. (1997). Solvent free protection of carbonyl group under microwave irradiation. Tetrahedron letters, 38(45), 7867-7870.

Schmidt, M., Ungvári, J., Glöde, J., Dobner, B., & Langner, A. (2007). New 1, 3-dioxolane and 1, 3-dioxane derivatives as effective modulators to overcome multidrug resistance. Bioorganic & medicinal chemistry, 15(6), 2283-2297.

Slaihim, M. M., Al-Suede, F. S. R., Khairuddean, M., Ahamed, M. B. K., & Majid, A. M. S. A. (2019). Synthesis, characterisation of new derivatives with mono ring system of 1, 2, 4-triazole scaffold and their anticancer activities. Journal of Molecular Structure, 1196, 78-87.

Slaihim, M. M., Al-Suede, F. S. R., Khairuddean, M., Sultan, S. B. S. H., Nazari, M., Ahamed, M. B. K., & Majid, A. M. S. A. (2023). Antitumor activity and synthesis of new derivatives with fused ring system of 1, 2, 4-triazole scaffold and their characterization. Journal of Molecular Structure, 1289, 135834.

Torok, D. S., Figueroa, J. J., & Scott, W. J. (1993). 1, 3-Dioxolane formation via Lewis acid-catalyzed reaction of ketones with oxiranes. The Journal of Organic Chemistry, 58(25), 7274-7276.

Wong, J. C., Sternson, S. M., Louca, J. B., Hong, R., & Schreiber, S. L. (2004). Modular synthesis and preliminary biological evaluation of stereochemically diverse 1, 3-dioxanes. Chemistry & biology, 11(9), 1279-1291.

Zeng, L., Xu, G., Gao, P., Zhang, M., Li, H., & Zhang, J. (2015). Design, synthesis and evaluation of a novel class of glucosamine mimetic peptides containing 1, 3-dioxane. European Journal of Medicinal Chemistry, 93, 109-120.